

NON-LINEAR ANALYSIS OF ACTIVE PRETWISTED ANISOTROPIC STRIPS

Ajay Kumar Tamrakar[†] and Dineshkumar Harursampath[‡]
 Department of Aerospace Engineering, Indian Institute of Science
 Bangalore-560012, INDIA

Abstract

Modeling of active anisotropic strips with small pretwist, based on the dimensional reduction of laminate shell theory to a non-linear one dimensional theory using variational asymptotic method is presented. The present paper treats the problem of designing an anisotropic beam actuator assuming all effective piezoelectric coefficients to be non-zero. Hence, direction of application of actuation electric field in the fiber can be optimized for higher actuation authority. This type of non-classical analysis is needed, for example, in problems, where trapeze effect is important, such as in active rotor blades. In order to demonstrate the usage of the results in the analysis of structures made of arbitrary geometrical combination of active pretwisted anisotropic strips, closed form expressions are derived for the performance of actuator corresponding to all directions of application of actuation electric fields. A numerical study is also conducted to investigate the effect of geometrical parameters on the performance of a twist actuator.

Symbols used

x_1 Cartesian coordinate along the axis of a strip
 x_i Cartesian coordinate for a cross section, $i = 2, 3$
 \mathbf{b}_i Unit vectors for undeformed geometry, $i = 1, 2, 3$
 \mathbf{B}_i Unit vectors for deformed geometry, $i = 1, 2, 3$
 Γ_{ij} 3-D Jaumann-Biot-Cauchy strains, $i, j = 1, 2, 3$
 E 3-D strains (linear part of Γ_{ij})
 σ_{ij} 3-D stresses, $i, j = 1, 2, 3$
 $\varepsilon_{\alpha\beta}$ 2-D membrane strains, $\alpha, \beta = 1, 2$
 $\rho_{\alpha\beta}$ 2-D elastic curvatures, $\alpha, \beta = 1, 2$
 A_{ij} 2-D membrane stiffness constants, $i, j = 1, 2, 6$
 B_{ij} 2-D coupling stiffness constants, $i, j = 1, 2, 6$
 D_{ij} 2-D bending stiffness constants, $i, j = 1, 2, 6$
 N_{ij} Laminate normal forces, $i, j = 1, 2$
 M_{ij} Laminate moments, $i, j = 1, 2$
 a Superscript for active properties
 γ_{11} 1-D axial strain
 κ_1 1-D elastic twist per unit length (twist rate)
 κ_i 1-D elastic bending curvatures, $i = 2, 3$
 \mathbf{S} 1-D stiffness matrix
 \bar{w}_i 3-D warping fields of cross section, $i = 1, 2, 3$
 w_i Warping averaged over strip/wall thickness, $i = 1, 2, 3$
 l Characteristic length of a beam
 b Characteristic dimension of a cross section
 h Thickness of a thin wall/strip
 k_1 Initial twist per unit length

ε Small parameter, magnitude of largest strain
 δ_h Small parameter, $\frac{h}{b}$
 δ_b Small parameter, $\frac{b}{l}$
 δ_t Small parameter, bk_1
 δ_R Small parameter, $\frac{R}{l}$
 Δ Small parameter, $\frac{\varepsilon}{\delta_h^2}$
 C_i^a Actuation coefficients, $i = 1, 2, 3$
 C_{ij} 3-D Stiffness coefficients $i, j = 1, 2, \dots, 6$
 c_i Coefficients for trapeze effect in the strip, $i = 1, 3$
 θ_o Initial twist in the strip
 E_i^a Actuation electric fields, $i = 1, 2, 3$

Introduction

In recent decades, researchers have been investigating the application of new material system developments to existing engineering systems in an effort to improve these systems. There is a drive towards systems with improved performance, less parts, lower maintenance cost and higher reliability. This paper focuses applications of new material technology to control mechanisms. In this view, there has been an increasing interest in the study of smart or intelligent structures. Actuators and sensors are two key components in these structures and Piezoelectric Fiber Reinforced Composite (PFRC) is one of the active materials which shows a lot of promise as an actuator. Modeling PFRC, also known as Active Fiber Composite (AFC), structures is the main focus of this paper. The actuator can be an AFC with Inter Digitated Electrodes (IDE) Ref [1]. This actuator concept provides a feasible way to integrally actuate the structure, as opposed to the use of the piezoceramic crystal patches, providing higher level of actuation authority.

Due to their geometry, high aspect ratio wings and helicopter rotors can often be treated as beams, that is, one dimensional bodies. This idealization of the structure leads to a much simpler mathematical formulation than would be obtained if complete three dimensional elastic formulation were used to model it. There is a significant amount of work in the literature dealing with capturing passive two dimensional (cross sectional) effects in beams. The concept of Variational Asymptotic Method (VAM) was introduced by V.L.Bedichevskii in 1978 Ref [20] for construction of theory of shells. VABS was developed by Cesnik and Hodges Ref [17] for modeling of composite beams. A non-linear closed-form analysis of anisotropic pretwisted strips including non-classical effects was presented in Ref [15].

Finite element based modeling of initially twisted and curved active composite beams was implemented through Active Variational Asymptotic Beam Section (VABS-A) analysis code by Cesnik and Morales Ref [2]. Also in Ref [2], the

[†]Post Graduate Student, E-mail: ajay@stc.iisc.ernet.in

[‡]Assistant Professor, Corresponding Author, Tel: 91-80-22933032, Fax: 91-80-23600134, E-mail:dinesh@aero.iisc.ernet.in

beam theory is formulated from geometrically non-linear 3 D elasticity. Cesnik and Shin have presented modeling of integrally actuated helicopter blades Ref [3] and asymptotic formulation for preliminary design of multiple-cell composite helicopter rotor blades with integral anisotropic active ply Ref [4]. A lot of experiments, design, manufacturing and testing of integrally twist actuated rotor blades have been accomplished Ref ([6] - [11]).

While good advances have been made in the field of passive cross-sectional modeling.

In general, piezoelectric composite materials are assumed to be homogeneous with effective electroelastic properties dependent upon the properties of its constituents, namely fiber and matrix materials and their concentrations in the composite. In order to tailor an AFC to the specific requirements of its role in a smart structure, it is essential to develop an efficient analytical model to predict its effective electroelastic properties and thus to investigate the effect of the composite constituents' properties and their micro-structural geometry on the overall composite properties.

Various micro-electromechanical models have been proposed for the effective properties of the AFC's Ref ([14] - [20]). If use of IDE Ref [1] and Circular Linked Interdigitated Electrodes (CLIDE) Ref [20] increase the cost and weight of the structure (a limitation in aerospace structures), then the most practical option is to apply the electric field across the thickness of the composite that is in a direction transverse to the fiber direction. Moreover, since the thickness of a layer of the composite is usually very small, it may not be difficult to maintain a constant electric field across the thickness of the composite. Piezoelectric constants of piezoelectric fibers depend upon their crystal structure and poling directions. Some constants are zero while some constants are equal to others. Effective piezoelectric coefficients of an AFC depend upon the piezoelectric constants of the constituent piezoelectric fiber. For an AFC to be used as an actuator or as a sensor, it is important to know which direction of application or measurement of the electric field in the fiber would be most effective for a particular composite and particular strain. Also, inspite of the flexibility for electrode configuration selection, all types of electrodes cannot be suitable for a particular AFC. Hence, in modeling of an arbitrary AFC, we need to generalize all piezoelectric coefficients to be non-zero, so that all components of the electric field can be accounted for in the model. For this general problem, no method has been proposed so far.

The work on AFC available in the literature is unable to predict specific properties required for design of AFC in applications for twist actuators using existing methods. Optimization of the design of an AFC actuator is expensive and lengthy. Hence, closed form expressions relating twist and all three components of the actuation electric field are required. Thus the objective of this analysis is to model a generally active pretwisted anisotropic strip for twist actuation with closed form derivations.

First, we reduce the 3D thin beam problem into a 2D shell problem by considering plane stress assumption and then reduce this further into 1D problem by taking the advantage of the presence of small parameters in the geometry of the strip. Resulting 1D strain energy density is a function only of x_1 (coordinate along the length). This dimensional reduction is done with the aid of variational asymptotic formulation (Berdichveskii [20]; Hodges [15]). After reducing it to a 1D problem, we effect the separation of material variables from the external actuation electric fields. In this way we can easily find the parameters affecting the actuation forces due to electric field components in any direction.

Analytical Development

The 3-D constitutive relations for a unidirectional AFC in its material coordinate system ($1^* - 2^* - 3^*$) is given by Eq.(1) as follows

$$\begin{Bmatrix} \sigma_{11}^* \\ \sigma_{22}^* \\ \sigma_{33}^* \\ \sigma_{23}^* \\ \sigma_{31}^* \\ \sigma_{12}^* \end{Bmatrix} = \mathbf{C}^* \begin{Bmatrix} \Gamma_{11}^* \\ \Gamma_{22}^* \\ \Gamma_{33}^* \\ 2\Gamma_{23}^* \\ 2\Gamma_{31}^* \\ 2\Gamma_{12}^* \end{Bmatrix} - \mathbf{e}^* \begin{Bmatrix} E_1^a \\ E_2^a \\ E_3^a \end{Bmatrix}, \quad (1)$$

where

$$\mathbf{C}^* = \begin{bmatrix} C_{11}^* & C_{12}^* & C_{13}^* & 0 & 0 & 0 \\ C_{12}^* & C_{22}^* & C_{23}^* & 0 & 0 & 0 \\ C_{13}^* & C_{23}^* & C_{33}^* & 0 & 0 & 0 \\ 0 & 0 & 0 & C_{44}^* & 0 & 0 \\ 0 & 0 & 0 & 0 & C_{55}^* & 0 \\ 0 & 0 & 0 & 0 & 0 & C_{66}^* \end{bmatrix}, \quad (2)$$

$$\mathbf{e}^* = \begin{bmatrix} e_{11}^* & e_{21}^* & e_{31}^* \\ e_{12}^* & e_{22}^* & e_{32}^* \\ e_{13}^* & e_{23}^* & e_{33}^* \\ e_{14}^* & e_{24}^* & e_{34}^* \\ e_{15}^* & e_{25}^* & e_{35}^* \\ e_{16}^* & e_{26}^* & e_{36}^* \end{bmatrix}. \quad (3)$$

Here σ^* , Γ^* , C^* and e^* are stress, strain, effective stiffness constants and effective piezoelectric stress constants in material coordinate system ($1^*-2^*-3^*$), respectively. E_1^a is the electric field component along the fiber length direction while E_2^a and E_3^a are the electric field components in mutually perpendicular directions, both of which are transverse to the fiber.

Plane stress assumption

The non-zero stresses for thin strip composite beams are the in plane normal stresses and shear stress in the laminate wall. The stresses in through thickness direction do exist but are relatively small. Therefore the problem can be treated as a plane stress problem with

$$\sigma_{33}^* = 0, \quad \sigma_{23}^* = 0 \quad \text{and} \quad \sigma_{31}^* = 0. \quad (4)$$

A static condensation process can be used in Eq.(1) to remove the effect of the stresses which are zero. The resulting ply

elastic constants \bar{Q}_{ij}^* 's and induced stress constants \bar{e}_{ij}^* 's are specifically for the plane stress problem and differ from the constants used for a complete 3-D analysis. Plane stress coefficients (stiffness and piezoelectric stress constants) are denoted with over bar. Note these equations are for the material coordinate system (1*-2*-3*) and still need to be related to the local beam wall coordinate system (1-2-3).

$$\begin{Bmatrix} \sigma_{11}^* \\ \sigma_{22}^* \\ \sigma_{12}^* \end{Bmatrix} = \bar{\mathbf{Q}}^* \begin{Bmatrix} \Gamma_{11}^* \\ \Gamma_{22}^* \\ 2\Gamma_{12}^* \end{Bmatrix} - \bar{\mathbf{e}}^* \begin{Bmatrix} E_1^a \\ E_2^a \\ E_3^a \end{Bmatrix}, \quad (5)$$

where

$$\bar{\mathbf{Q}}^* = \begin{bmatrix} \bar{Q}_{11}^* & \bar{Q}_{12}^* & 0 \\ \bar{Q}_{12}^* & \bar{Q}_{22}^* & 0 \\ 0 & 0 & \bar{Q}_{66}^* \end{bmatrix}, \quad (6)$$

$$\bar{\mathbf{e}}^* = \begin{bmatrix} \bar{e}_{11}^* & \bar{e}_{21}^* & \bar{e}_{31}^* \\ \bar{e}_{12}^* & \bar{e}_{22}^* & \bar{e}_{32}^* \\ \bar{e}_{16}^* & \bar{e}_{26}^* & \bar{e}_{36}^* \end{bmatrix}. \quad (7)$$

Elements of $\bar{\mathbf{Q}}^*$ and $\bar{\mathbf{e}}^*$ are given as follows

$$\bar{Q}_{11}^* = C_{11}^* - \frac{C_{13}^{*2}}{C_{33}^*}, \quad \bar{Q}_{12}^* = C_{12}^* - \frac{C_{13}^* C_{23}^*}{C_{33}^*},$$

$$\bar{Q}_{22}^* = C_{22}^* - \frac{C_{23}^{*2}}{C_{33}^*}, \quad \bar{Q}_{66}^* = C_{66}^*,$$

and

$$\bar{e}_{11}^* = e_{11}^* - \frac{C_{13}^* e_{13}^*}{C_{33}^*}, \quad \bar{e}_{21}^* = e_{21}^* - \frac{C_{13}^* e_{23}^*}{C_{33}^*}, \quad \bar{e}_{31}^* = e_{31}^* - \frac{C_{13}^* e_{33}^*}{C_{33}^*},$$

$$\bar{e}_{12}^* = e_{12}^* - \frac{C_{23}^* e_{13}^*}{C_{33}^*}, \quad \bar{e}_{22}^* = e_{22}^* - \frac{C_{23}^* e_{23}^*}{C_{33}^*}, \quad \bar{e}_{32}^* = e_{32}^* - \frac{C_{23}^* e_{33}^*}{C_{33}^*},$$

$$\bar{e}_{16}^* = e_{16}^*, \quad \bar{e}_{26}^* = e_{26}^*, \quad \bar{e}_{36}^* = e_{36}^*.$$

Property rotation

The plane stress constitutive Eq.(5) are for the coordinate system which is aligned along with the principal material property axis system (1*-2*-3*). To obtain the correct material properties in the structural coordinate system (1-2-3), the material properties must be rotated according to the tensor transformation laws. The relative location of the structural axis and the material axis system is shown in Fig. 1.

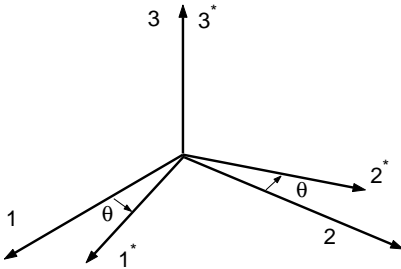


Fig 1. Material coordinate system (1*-2*-3*) and structural coordinate system (1-2-3)

The stress and strain transformation matrix from (1*-2*-3*) material system to the (1-2-3) local coordinate system is given by

$$\mathbf{T} = \begin{bmatrix} \cos^2 \theta & \sin^2 \theta & -2 \sin \theta \cos \theta \\ \sin^2 \theta & \cos^2 \theta & 2 \sin \theta \cos \theta \\ \sin \theta \cos \theta & -\sin \theta \cos \theta & \cos^2 \theta - \sin^2 \theta \end{bmatrix}, \quad (8)$$

where θ is the angle between axes 1* and 1 in right handed system to be positive (see Fig. 1). So stresses in the structural coordinate system (1-2-3) are given by

$$\begin{Bmatrix} \sigma_{11} \\ \sigma_{22} \\ \sigma_{12} \end{Bmatrix} = \mathbf{T} \begin{Bmatrix} \sigma_{11}^* \\ \sigma_{22}^* \\ \sigma_{12}^* \end{Bmatrix}. \quad (9)$$

Because induced stress constants \bar{e}_{ij}^* 's are just the plane stresses when multiplied with the actuation electric field components, induced stress constants \bar{e}_{ij} 's in structural coordinate system (1-2-3) are given by

$$\bar{\mathbf{e}} = \begin{bmatrix} \bar{e}_{11} & \bar{e}_{21} & \bar{e}_{31} \\ \bar{e}_{12} & \bar{e}_{22} & \bar{e}_{32} \\ \bar{e}_{16} & \bar{e}_{26} & \bar{e}_{36} \end{bmatrix} = \mathbf{T} \begin{bmatrix} \bar{e}_{11}^* & \bar{e}_{21}^* & \bar{e}_{31}^* \\ \bar{e}_{12}^* & \bar{e}_{22}^* & \bar{e}_{32}^* \\ \bar{e}_{16}^* & \bar{e}_{26}^* & \bar{e}_{36}^* \end{bmatrix}. \quad (10)$$

Let $\bar{\mathbf{Q}}$ represents the stiffness matrix in the (1-2-3) structural coordinate system, expanded as

$$\bar{\mathbf{Q}} = \begin{bmatrix} \bar{Q}_{11} & \bar{Q}_{12} & \bar{Q}_{16} \\ \bar{Q}_{12} & \bar{Q}_{22} & \bar{Q}_{26} \\ \bar{Q}_{16} & \bar{Q}_{26} & \bar{Q}_{66} \end{bmatrix}. \quad (11)$$

It should be noted here that stiffness matrix $\bar{\mathbf{Q}}$ is symmetric but stress constant matrix $\bar{\mathbf{e}}$ is not symmetric. By using tensor transformation rules and constant energy density function, we find

$$\bar{\mathbf{Q}} = \mathbf{T} \bar{\mathbf{Q}}^* \mathbf{H} \mathbf{T}^{-1} \mathbf{H}^{-1}, \quad (12)$$

where

$$\mathbf{H} = \begin{bmatrix} 1 & 0 & 0 \\ 0 & 1 & 0 \\ 0 & 0 & 2 \end{bmatrix}. \quad (13)$$

Here \mathbf{H} is the Reuter matrix that transforms tensor strains into engineering strains. Expressions for \bar{Q}_{ij} 's and \bar{e}_{ij} 's are given in the appendix. Hence, constitutive relations for an AFC lamina reduce from 3-D to 2-D and take the following form

$$\begin{Bmatrix} \sigma_{11} \\ \sigma_{22} \\ \sigma_{12} \end{Bmatrix} = \bar{\mathbf{Q}} \begin{Bmatrix} \Gamma_{11} \\ \Gamma_{22} \\ 2\Gamma_{12} \end{Bmatrix} - \bar{\mathbf{e}} \begin{Bmatrix} E_1^a \\ E_2^a \\ E_3^a \end{Bmatrix}. \quad (14)$$

It should be noted here that electrical fields E_i^a in Eq.(14) are in the material coordinate system. Hence, E_1^a denotes electric field along the length of the fibers, E_2^a and E_3^a are electrical field components transverse to the fiber length direction.

Active Laminated Plate Theory

In the Classical Laminated Plate Theory (CLPT), it is assumed that the strains vary linearly with the thickness of the laminate for the proper bonding between laminates. Hence, we have the following expression for strains

$$\begin{Bmatrix} \Gamma_{11} \\ \Gamma_{22} \\ 2\Gamma_{12} \end{Bmatrix} = \begin{Bmatrix} \varepsilon_{11} \\ \varepsilon_{22} \\ 2\varepsilon_{12} \end{Bmatrix} + x_3 \begin{Bmatrix} \rho_{11} \\ \rho_{22} \\ 2\rho_{12} \end{Bmatrix}, \quad (15)$$

where ε_{11} , ε_{22} and ε_{12} are mid plane tensor strains, x_3 is the distance of a generic material point from the mid plane (positive in direction-3) and ρ_{11} , ρ_{22} and $2\rho_{12}$ are the midplane elastic curvatures.

Expressions for Γ_{11} , Γ_{22} and Γ_{12} from Eq.(15) are substituted in Eq.(14) to find σ_{11} , σ_{22} and σ_{12} . CLPT forces and moments are related to the plane stresses as follows

$$\{N_{11}, N_{22}, N_{12}\} = \int_{-\frac{h}{2}}^{\frac{h}{2}} \{\sigma_1, \sigma_2, \sigma_{12}\} dx_3, \quad (16)$$

$$\{M_{11}, M_{22}, M_{12}\} = \int_{-\frac{h}{2}}^{\frac{h}{2}} \{\sigma_1, \sigma_2, \sigma_{12}\} x_3 dx_3. \quad (17)$$

Expressions for N_{ij} and M_{ij} are written in a matrix form as

$$\begin{Bmatrix} N_{11} \\ N_{22} \\ N_{12} \\ M_{11} \\ M_{22} \\ M_{12} \end{Bmatrix} = \begin{bmatrix} \mathbf{A} & \mathbf{B} \\ \mathbf{B} & \mathbf{D} \end{bmatrix} \begin{Bmatrix} \varepsilon_{11} \\ \varepsilon_{22} \\ 2\varepsilon_{12} \\ \rho_{11} \\ \rho_{22} \\ 2\rho_{12} \end{Bmatrix} - \begin{Bmatrix} N_{11}^a \\ N_{22}^a \\ N_{12}^a \\ M_{11}^a \\ M_{22}^a \\ M_{12}^a \end{Bmatrix}. \quad (18)$$

Here A_{ij} , B_{ij} and D_{ij} are laminate stiffness coefficients defined as

$$\{A_{ij}, B_{ij}, D_{ij}\} = \int_{-\frac{h}{2}}^{\frac{h}{2}} \bar{Q}_{ij} \{dx_3, x_3 dx_3, x_3^2 dx_3\}. \quad (19)$$

N_{ij}^a and M_{ij}^a are the actuation forces and actuation moments (similar to N_{ij} and M_{ij}) given by

$$\begin{Bmatrix} N_{11}^a \\ N_{22}^a \\ N_{12}^a \\ M_{11}^a \\ M_{22}^a \\ M_{12}^a \end{Bmatrix} = \begin{bmatrix} A_{11}^a & A_{21}^a & A_{31}^a \\ A_{12}^a & A_{22}^a & A_{32}^a \\ A_{16}^a & A_{26}^a & A_{36}^a \\ B_{11}^a & B_{21}^a & B_{31}^a \\ B_{12}^a & B_{22}^a & B_{32}^a \\ B_{16}^a & B_{26}^a & B_{36}^a \end{bmatrix} \begin{Bmatrix} E_1^a \\ E_2^a \\ E_3^a \end{Bmatrix}. \quad (20)$$

A_{ij}^a and B_{ij}^a in Eq.(20) are the active laminate stress constants, defined as

$$\{A_{ij}^a, B_{ij}^a\} = \int_{-\frac{h}{2}}^{\frac{h}{2}} \bar{e}_{ij} \{dx_3, x_3 dx_3\}. \quad (21)$$

For symmetric laminates: For symmetric laminates, we have

$$B_{ij} = 0, \quad B_{ij}^a = 0 \quad (22)$$

resulting in neither bending-extension coupling nor twist extension coupling as well as the inability to actuate bending or torsion in the shells. For antisymmetric laminates, we have

$$A_{16} = A_{26} = B_{11} = B_{12} = B_{22} = B_{66} = D_{16} = D_{26} = 0. \quad (23)$$

along with

$$B_{i1}^a = B_{i2}^a = 0 \quad (i = 1, 2, 3) \quad (24)$$

indicating the inability to actuate shell bending.

Kinematics

Asymptotic method requires small parameters. Here the wavelength of the deformation along the strip is denoted by l . The width and thickness of the strip are denoted by b and h respectively. From the geometry of the strip, the natural and small parameters are the thickness-to-width ratio $\delta_h = h/b$; the width-to-length ratio $\delta_b = b/l$; and the width times pretwist per unit length $\delta_t = bk_1$, where k_1 is the derivative of the pretwist angle with respect to the length along the strip. The geometry of the strip is shown in the Fig. 2.

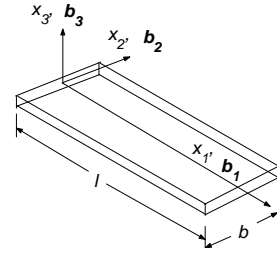


Fig. 2. Active pretwisted strip configuration and coordinate system

The Cartesian coordinate measures x_i are directed along the length, width and thickness of the strip for $i = 1, 2$ and 3 respectively, parallel to corresponding unit vectors \mathbf{b}_i . Here the strip has the pretwist rate $k_1(x_1)$, so that the unit vectors associated with the cross-sectional plane \mathbf{b}_2 and \mathbf{b}_3 , are functions of x_1 . The position vector from a point fixed in an inertial reference frame to a generic point on the middle surface of the strip is $\mathbf{r} = x_1 \mathbf{b}_1 + x_2 \mathbf{b}_2(x_1)$. The position vector of an arbitrary material point in the strip is then

$$\check{\mathbf{r}} = \mathbf{r} + x_3 \mathbf{b}_3(x_1) = x_i \mathbf{b}_i. \quad (25)$$

The covariant base vectors \mathbf{g}_i are tangent to the coordinate curves [18]:

$$\mathbf{g}_i(x_1, x_2, x_3) = \frac{\partial \check{\mathbf{r}}}{\partial x_i}. \quad (26)$$

Contravariant base vectors can be obtained by standard means as

$$\mathbf{g}^i(x_1, x_2, x_3) = \frac{e_{ijk} \mathbf{g}_j \times \mathbf{g}_k}{2\sqrt{g}}. \quad (27)$$

Here g is given by

$$g = \det(\mathbf{g}_i \cdot \mathbf{g}_j). \quad (28)$$

and e_{ijk} are the components of the permutation tensor in Cartesian coordinate system. (Repeated indices are always summed up over their ranges.)

Before applying VAM, we will formulate the kinematics of the problem using the procedure outlined by Danielson and Hodges [18]. The position vector of an arbitrary material point in the deformed configuration [15] is given by

$$\check{\mathbf{R}} = x_1 \mathbf{b}_1 + u_i(x_1) \mathbf{b}_i + x_2 \mathbf{B}_2(x_1) + x_3 \mathbf{B}_3(x_1) + \bar{w}_i(x_1, x_2, x_3) \mathbf{B}_i(x_i), \quad (29)$$

where u_i are rigid body displacements; \mathbf{B}_i are orthogonal unit vectors introduced by rigid body rotation; and \bar{w}_i are warping displacements of the beam cross-section.

Based on the main exchange rules in [19] and recovery relations in [20], \bar{w}_3 the warping displacement component that is normal to the local shell can be split into two parts: an average across the thickness $w_3(x_1, x_2)$ and an unknown variation due to Poisson like effects. The shell inplane warping components (\bar{w}_1, \bar{w}_2) are split into three parts each, the additional part being due to local rotations. The warping displacements are governed by the constraints [15]

$$\langle w_i \rangle = 0, \quad \langle w_{3,2} \rangle = 0, \quad (30)$$

with the notation

$$\langle \bullet \rangle = \int_{-b/2}^{b/2} \bullet dx_2 \quad (31)$$

being used.

The covariant base vectors \mathbf{G}_i are tangent to the coordinate curves of the deformed strip [18] and are given by

$$\mathbf{G}_i(x_1, x_2, x_3) = \frac{\partial \tilde{\mathbf{R}}}{\partial x_i}. \quad (32)$$

We can now evaluate the Deformation Gradient Tensor (DGT) $\mathbf{A} = \mathbf{G}_i \mathbf{g}^i$. The VAM can be applied in an iterative manner, where a preliminary order of magnitude analysis is used to develop a somewhat arbitrary estimation scheme. At the end of the first step of applying the method, the results are checked to see if they are actually of the assumed order. If not, an additional step must be taken to obtain asymptotically correct results, as suggested in [20]. Here, for preliminary step, we note that all the 3-D strains E_{ij} are $O(\varepsilon)$. At this step, for a strip of our problem, the orders of different variables are estimated by using the expressions for E_{ij} [15] as follows

$$w_\alpha = O(\varepsilon b), \quad \alpha = 1, 2, \quad w_3 = O\left(\frac{\varepsilon b}{\delta_h}\right),$$

$$\gamma_{11} = O(\varepsilon), \quad \kappa_\alpha = O\left(\frac{\varepsilon}{\delta_h b}\right), \quad \kappa_3 = O\left(\frac{\varepsilon}{b}\right).$$

Here γ_{11} , κ_i are 1-D strain measures. By using kinematic formulation with continuum mechanics, for a pretwisted strip, it has been shown that the 3-D strain Γ (using the moderate local rotation approximation [18]) are given by

$$\Gamma = E - \frac{\tilde{A}^2}{2} + \frac{E\tilde{A} - \tilde{A}E}{2}, \quad (33)$$

where \tilde{A} is anti symmetric component of deformation gradient tensor A given by

$$\tilde{A} = \frac{A - A^T}{2}, \quad (34)$$

and E is the linear part of Jaumann-Biot-Cauchy strain (to be used if small local rotations were assumed, but *not* the assumption made at here) given by

$$E = \frac{A + A^T}{2} - I_3. \quad (35)$$

The 3-D strain components that are of further interest to us are

$$\Gamma_{11} = \underbrace{\gamma_{11} - x_2 \kappa_3 + x_3 \kappa_2}_{O(\varepsilon)} + \underbrace{k_1 x_2^2 \kappa_1}_{O(\varepsilon \delta_t / \delta_h)} + \underbrace{\frac{x^2 \kappa_1^2}{2} + w_3 \kappa_2}_{O(\frac{\varepsilon^2}{\delta_h^2})} + O\left(\varepsilon \delta_b, \varepsilon \delta_t, \frac{\varepsilon^2}{\delta_b}\right), \quad (36)$$

$$\Gamma_{22} = \underbrace{w_{2,2} - x_3 w_{3,22}}_{O(\varepsilon)} + \underbrace{\frac{1}{2} w_{3,2}^2}_{O(\frac{\varepsilon^2}{\delta_h^2})} + O(\varepsilon \delta_h), \quad (37)$$

$$2\Gamma_{12} = \underbrace{w_{1,2} - 2x_3 \kappa_1}_{O(\varepsilon)} + \underbrace{k_1(x_2 w_{3,2} - w_3)}_{O(\varepsilon \delta_t / \delta_h)} + \underbrace{\kappa_1(x_2 w_{3,2} - w_3)}_{O(\frac{\varepsilon^2}{\delta_h^2})} + O\left(\varepsilon \delta_b, \varepsilon \delta_h, \varepsilon \delta_t, \frac{\varepsilon^2}{\delta_h}\right). \quad (38)$$

Since δ 's are small parameters, we ought to retain the terms of $O(\varepsilon \delta_t / \delta_h)$ in comparison to the terms of $O(\varepsilon)$. Furthermore, the terms of $O(\varepsilon^2 / \delta_h^2)$ assume significance. Denoting the ratio ε / δ_h^2 by the small parameters Δ , we note that the zeroth order approximation should contain all the terms up to $O(E\varepsilon^2\Delta^2)$, where a typical stiffness coefficient is $O(E)$. This in turn means that the zeroth order approximation to the strains should contain all the relevant terms up to $O(\varepsilon\Delta^2)$. On the other hand, terms of $O(\varepsilon\delta_b)$, $O(\varepsilon\delta_h)$, $O(\varepsilon\delta_t)$ and $O(\varepsilon^2/\delta_h^2)$ can be included in the higher order approximation, if necessary.

3-D strain measures are related to 2-D strain measures by Eq.(15). Hence, by inspection of the Eqs. (36-38), we obtain the relation between 2-D (shell) measures and 1-D (beam) measures. The membrane strains are

$$\varepsilon_{11} \approx \gamma_{11} - x_2 \kappa_3 + k_1 x_2^2 \kappa_1 + \frac{x^2 \kappa_1^2}{2} + \underline{w_3 \kappa_2}, \quad (39)$$

$$\varepsilon_{22} \approx w_{2,2} + \underline{\frac{1}{2} w_{3,2}^2}, \quad (40)$$

$$2\varepsilon_{12} \approx w_{1,2} + k_1(x_2 w_{3,2} - w_3) + \underline{\kappa_1(x_2 w_{3,2} - w_3)}, \quad (41)$$

while the midplane elastic curvatures are

$$\rho_{11} \approx \kappa_2, \quad (42)$$

$$\rho_{22} \approx -w_{3,22}, \quad (43)$$

$$2\rho_{12} \approx -2\kappa_1. \quad (44)$$

In the above equations, the underlined terms (of the order of ε^2/δ_h^2) are non-linear and arise due to moderate local rotations. The non-underlined terms (of the order of ε or $\varepsilon\delta_t/\delta_h$) in these equations are the dominant ones, the only ones needed for the zeroth order approximation. The first-order approximation should include all the above terms. Here as a preliminary step, $A_{ij}^a E_i^a$ and $B_{ij}^a E_i^a$ are assumed to be of the order higher than $O(E\varepsilon h)$ and $O(E\varepsilon h^2)$ respectively which can be considered as putting an upper limit on the applied electric field magnitude.

Strain Energy of the Active strip

Now we consider the strip to be a 2-D elastic body. Its strain energy density (i.e. energy per unit middle surface area) is given by

$$U_{2D} = \frac{1}{2} \begin{Bmatrix} \varepsilon \\ \rho \end{Bmatrix}^T \left\{ \begin{bmatrix} \mathbf{A} & \mathbf{B} \\ \mathbf{B} & \mathbf{D} \end{bmatrix} \begin{Bmatrix} \varepsilon \\ \rho \end{Bmatrix} - \begin{bmatrix} \mathbf{A}^a \\ \mathbf{B}^a \end{bmatrix} \mathbf{E}^a \right\}, \quad (45)$$

where

$$\begin{Bmatrix} \varepsilon \\ \rho \end{Bmatrix} = \begin{Bmatrix} \varepsilon_{11} \\ \varepsilon_{22} \\ 2\varepsilon_{12} \\ \rho_{11} \\ \rho_{22} \\ 2\rho_{12} \end{Bmatrix}, \quad \mathbf{E}^a = \begin{Bmatrix} E_1^a \\ E_2^a \\ E_3^a \end{Bmatrix}. \quad (46)$$

Zeroth-order approximation

The zeroth order approximation to the 2-D strain energy density consists of all the terms of $O(E\varepsilon^2)$ thus leading to the asymptotic classical linear theory for general active anisotropic pretwisted rectangular strips. Hence the zeroth order approximations to the 2-D membrane and bending strains are all of the non-underlined terms in the Eqs. (39-44). All the zeroth order variables will be denoted by a superscript 0. Minimization of U_{2D} with respect to ε_{12}^0 (the only strain measure which has a w_1^0 -dependent term) and ε_{22}^0 (the only strain measure which has a w_2^0 -dependent term) in turn means that N_{12} and N_{22} are zero. We reduce the active laminate plate theory (Eq.(18)) matrix by employing a process similar to the one applied for the condensation of the 3-D problem into a plane stress problem and get condensed equations in a more convenient form that separates material properties from external variables as follows

$$\begin{Bmatrix} N_{11} \\ M_{11} \\ M_{22} \\ M_{12} \end{Bmatrix} = \begin{bmatrix} \bar{\mathbf{A}} & \bar{\mathbf{B}} \\ \bar{\mathbf{B}} & \bar{\mathbf{D}} \end{bmatrix} \begin{Bmatrix} \varepsilon_{11} \\ \rho_{11} \\ \rho_{22} \\ 2\rho_{12} \end{Bmatrix} - \begin{bmatrix} \bar{\mathbf{A}}^a \\ \bar{\mathbf{B}}^a \end{bmatrix} \mathbf{E}^a. \quad (47)$$

where

$$\begin{bmatrix} \bar{\mathbf{A}} & \bar{\mathbf{B}} \\ \bar{\mathbf{B}} & \bar{\mathbf{D}} \end{bmatrix} = \begin{bmatrix} \bar{A}_{11} & \bar{B}_{11} & \bar{B}_{12} & \bar{B}_{16} \\ \bar{B}_{11} & \bar{D}_{11} & \bar{D}_{12} & \bar{D}_{16} \\ \bar{B}_{12} & \bar{D}_{12} & \bar{D}_{22} & \bar{D}_{26} \\ \bar{B}_{16} & \bar{D}_{16} & \bar{D}_{26} & \bar{D}_{66} \end{bmatrix}, \quad (48)$$

$$\begin{bmatrix} \bar{\mathbf{A}}^a \\ \bar{\mathbf{B}}^a \end{bmatrix} = \begin{bmatrix} \bar{A}_{11}^a & \bar{A}_{21}^a & \bar{A}_{31}^a \\ \bar{B}_{11}^a & \bar{B}_{21}^a & \bar{B}_{31}^a \\ \bar{B}_{12}^a & \bar{B}_{22}^a & \bar{B}_{32}^a \\ \bar{B}_{16}^a & \bar{B}_{26}^a & \bar{B}_{36}^a \end{bmatrix}. \quad (49)$$

New stiffness and stress coefficients, with over bar, used in above relations are defined in the appendix. U_{2D} is minimized with respect to ρ_{22} , and it is solved for ρ_{22} , then w_3^0 is calculated by using the constraint Eq.(30). Similarly, w_α^0 are also calculated. Thus, minimization of the zeroth order strain energy leads to ε_{12}^0 , ε_{22}^0 and ρ_{22}^0 being expressed in terms of the other known 2-D strain measures. Closed form solutions are thus obtained for the zeroth-order warping displacements w_i^0 and it is verified that their orders of magnitude agree with our estimations. For example, the shell out-of-plane warping is given by

$$w_3^0 = (12x_2^2 - b^2) \frac{\bar{B}_{12}\gamma_{11} + \bar{D}_{12}\kappa_2 - 2\bar{D}_{26}\kappa_1}{24\bar{D}_{22}} + x_2(b^2 - 4x_2^2) \frac{\bar{B}_{12}\kappa_3}{24\bar{D}_{22}} + (80x_2^4 - b^4) \frac{\bar{B}_{12}\kappa_1\kappa_1}{960\bar{D}_{22}}. \quad (50)$$

First-order approximation

The first-order approximation to the 2-D strain energy consists of all terms of $O(E\varepsilon^2)$, $O(E\varepsilon^2\Delta)$, $O(E\varepsilon^2\Delta^2)$. Hence the first-order approximations to the 2-D strains should contain all the terms up to $O(\varepsilon\Delta^2)$. This consists of both the underlined and non-underlined terms in the Eqs. (39-44). First-order variables will be denoted by superscript I . The warping displacements are given by $w_i^I = w_i^0 + \tilde{w}_i$, where the perturbation quantities \tilde{w}_i are assumed to be of an order higher than the corresponding zeroth order quantities w_i^0 . Thus $\tilde{w}_\alpha = O(\varepsilon\Delta b)$ and $\tilde{w}_3 = O(\varepsilon\Delta b/\delta_h)$.

Terms of order higher than $O(E\varepsilon^2\Delta^2)$ are excluded from the energy expression. With the help of lagrange multipliers, minimization of first-order strain energy is conducted. Closed form solutions are then obtained for perturbations to the zeroth-order warping displacements and it is verified that their orders of magnitude agree with our estimations. The 1-D strain energy density (energy per unit length) is given by

$$U_{1D} = \int_{-b/2}^{b/2} U_{2D} dx_2. \quad (51)$$

In order to carry out integration of Eq.(51) we need only shell out of plane warping field w_3 that has been determined through zeroth and first order approximations. Substitution of w_3^I for w_3 in the expression for U_{2D} with reduced stiffness matrix, we obtain the 1-D strain energy density from Eq.(51) as

$$U_{1D} = \frac{1}{2} \varepsilon_{ln}^T [\mathbf{S}]_{9 \times 9} \varepsilon_{ln} - \begin{Bmatrix} \gamma_{11} \\ \kappa_1 \\ \kappa_2 \\ \kappa_1^2 \\ \kappa_1\kappa_2 \end{Bmatrix}^T \mathbf{S}^a \begin{Bmatrix} E_1^a \\ E_2^a \\ E_3^a \end{Bmatrix}, \quad (52)$$

where

$$\mathbf{S}^a = \begin{bmatrix} S_{11}^a & S_{21}^a & S_{31}^a \\ S_{12}^a & S_{22}^a & S_{32}^a \\ S_{13}^a & S_{23}^a & S_{33}^a \\ S_{14}^a & S_{24}^a & S_{34}^a \\ S_{15}^a & S_{25}^a & S_{35}^a \end{bmatrix} \quad \text{and}$$

$$\varepsilon_{ln} = \{ \gamma_{11} \ \kappa_1 \ \kappa_2 \ \kappa_3 \ \kappa_1^2 \ \kappa_2^2 \ \kappa_2\gamma_{11} \ \kappa_2\kappa_3 \ \kappa_2\kappa_1 \ }^T.$$

Expression for S_{ij} and S_{ij}^a are given in the appendix. It should be noted here that ε_{ln} contains linear and non-linear terms of strains and also the strains in the actuation terms contain non-linear terms. Here the stiffness matrix \mathbf{S} is symmetric.

Application

In order to evaluate the developed analytical model, we study the special case of cantilevered laminated strip with antisymmetric layup loaded only by an axial force at the tip. The reason for the selection of this specialized case was two-fold. Antisymmetric layups produce laminates with extension-twist coupling; the non-linear coupling between extension and twist is one of the predominant non-linear effects. Secondly antisymmetric layups have been used in twist actuation recently (Ref [2]-Ref [3]). For antisymmetric laminates, the definitions for the stiffness coefficients with a bar are greatly simplified because Eq.(23) results in

$$\bar{B}_{11} = \bar{B}_{12} = \bar{D}_{16} = \bar{D}_{26} = 0, \quad (53)$$

and decoupling of bending in both directions from extension and twist. The equilibrium equations are derived via the principle of virtual work. First, the strain energy is given as

$$U = \int_0^l U_{1D}(\gamma_{11}, \kappa_1, \kappa_2, \kappa_3, E_1^a, E_2^a, E_3^a) dx_1. \quad (54)$$

The principle of virtual work for an axially loaded strip can be written as

$$\delta U = F_1 \delta u_1(l), \quad (55)$$

where F_1 is the axial load applied at the tip $x_1 = l$. For the case of an antisymmetric layup under an axial force, both κ_2 and κ_3 are zero. The geometrically exact strain-displacement relations reduce to $\gamma_{11} = u_1'$ and $\kappa_1 = \theta_1'$, where θ_1 is the elastic angle of twist. The two governing equilibrium equations thus reduce to algebraic equations for the coupled extension-twist problem:

$$\frac{\partial U_{1D}}{\partial \gamma_{11}} = F_1, \quad \frac{\partial U_{1D}}{\partial \kappa_1} = 0. \quad (56)$$

These equations are solved by using the first equation to eliminate γ_{11} in favour of F_1 and then using the second to express F_1 in terms of κ_1 . For constant k_1 , the tip pretwist angle $\theta_0 = lk_1$ and κ_1 is also a constant so that the elastic tip twist angle $\theta_t = l\kappa_1$. The result is

$$F_1 = \frac{[c_1 + c_2(\theta_t^2 + 3\theta_t\theta_0 + 2\theta_0^2)]\theta_t - C_i^a E_i^a}{c_3 - (\theta_t + \theta_0)}, \quad (57)$$

where

$$c_1 = \frac{48}{b} \left(\bar{D}_{66} - \frac{\bar{B}_{16}^2}{\bar{A}_{11}} \right), \quad c_2 = \frac{b^3 \bar{A}_{11}}{30l^2}, \quad c_3 = \frac{24l \bar{B}_{16}}{b^2 \bar{A}_{11}}, \quad (58)$$

$$C_i^a = \frac{b \bar{A}_{i1}^a c_3}{2} - \frac{12l \bar{B}_{i6}^a}{b}, \quad (i = 1, 2, 3) \quad (59)$$

It is observed that the contribution from the c_2 term is negligible in comparison to that of the c_1 term. As a result the extension-twist relation developed above takes the following simple form:

$$F_1 = \frac{c_1 \theta_t - C_1^a E_1^a - C_2^a E_2^a - C_3^a E_3^a}{c_3 - (\theta_t + \theta_0)}. \quad (60)$$

Eq.(60) represents the relation between the twist induced, axial force and actuation electric fields in all three directions. Coefficients c_1 and c_3 represent the coupling between axial force and twist responsible for the trapeze effect. One can observe that constants C_1^a , C_2^a and C_3^a are material dependent properties and represent the performance of the twist actuator. From Eq.(60), expression for twist generated due to axial force F_1 and actuation electric field components E_i^a can be written as

$$\theta_t = \frac{(c_3 - \theta_0) F_1 + C_1^a E_1^a + C_2^a E_2^a + C_3^a E_3^a}{(c_1 + F_1)}. \quad (61)$$

Pretwist θ_0 in the strip affects twist actuation authority, because

$$\frac{\partial \theta_t}{\partial \theta_0} = \frac{-F_1}{(c_1 + F_1)}. \quad (62)$$

From Eq.(62), it is clear that in the absence of axial force F_1 , pretwist in the strip does not have any effect on the twist actuation.

Numerical Study

To investigate the effects of the orientation of the piezoelectric fiber in the antisymmetric laminates, we consider a laminate with layup [AFC(PZT-5H/Epoxy)+ α° /AFC (PZT-5H/Epoxy) - α°], where α is fiber orientation angle and thickness of each lamina is 0.127 mm. Material properties are (L and T denote lateral and transverse properties respectively): $E_L = 42.2 \text{ GPa}$, $E_T = 17.5 \text{ GPa}$, $G_{LT} = 5.5 \text{ GPa}$, $\nu_{LT} = 0.354$, $d_{11} = 381 \text{ pm/V}$, $d_{12} = -160 \text{ pm/V}$, distance between electrodes in IDE = 1.143 mm as given

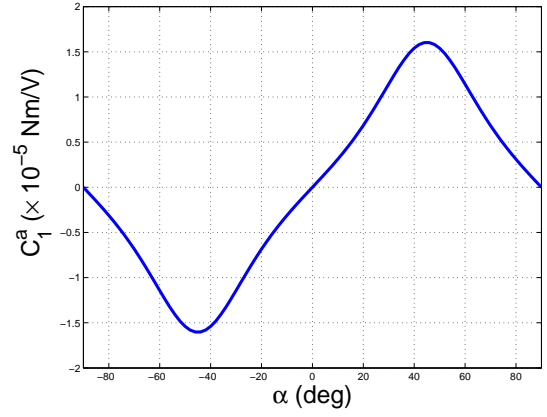


Fig. 3. Variation of C_1^a with fiber orientation angle α

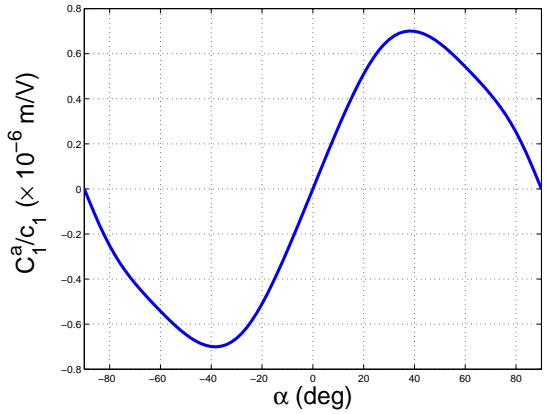


Fig. 4. Variation of $\frac{C_1^a}{c_1}$ with fiber orientation angle α

in [2]. Piezoelectric stress constant matrix \mathbf{e} is calculated by relation $\mathbf{e} = \mathbf{Q} \cdot \mathbf{d}$. Material properties in terms of plane stress stiffness coefficients \bar{Q}_{ij}^* and piezoelectric constants \bar{e}_{ij}^* are $\bar{Q}_{11}^* = 44.513 \text{ GPa}$, $\bar{Q}_{12}^* = 6.535 \text{ GPa}$, $\bar{Q}_{22}^* = 18.459 \text{ GPa}$, $\bar{Q}_{66}^* = 5.50 \text{ GPa}$, $\bar{e}_{11}^* = 15.914 \text{ N/Vm}$, $\bar{e}_{12}^* = -0.4638 \text{ N/Vm}$. laminate active length is $l = 0.374 \text{ m}$ and width is $b = 0.025 \text{ m}$. Same electrical fields are applied in both the active layers. From Eq.(60), it is found that in designing a twist actuator, C_i^a are most important parameters. There is no coupling between the transverse components of the electrical field (*i.e.* E_2^a , E_3^a) and the twist actuated for the chosen configuration. Hence, for the laminate under numerical study, one can interpret that only an electric field along the fiber length can produce twist actuation. This has been proved by the present analysis because actuation coefficients C_2^a and C_3^a are zero for the material and layup considered. Only non-zero actuation coefficient is C_1^a which is dependent upon the fiber orientation angle α . Fig. 3 shows that $|C_1^a|$ is maximum when $\alpha \pm 45^\circ$ and zero for $\alpha = 0^\circ$ and 90° . This proves that symmetric laminates cannot produce twist actuation. For the AFC materials with e_{31} and e_{32} non-zero, it can be shown that C_3^a is maximum when $\alpha = 45^\circ$ and zero for $\alpha = 0^\circ$, 90° and 180° . In the absence of axial force, the twist actuated per unit length will be given by

$$\theta_t = \frac{C_1^a E_1^a + C_2^a E_2^a + C_3^a E_3^a}{c_1}. \quad (63)$$

For the material considered, only E_1^a is effective for twist actuation. For the optimum design of twist actuator, it be-

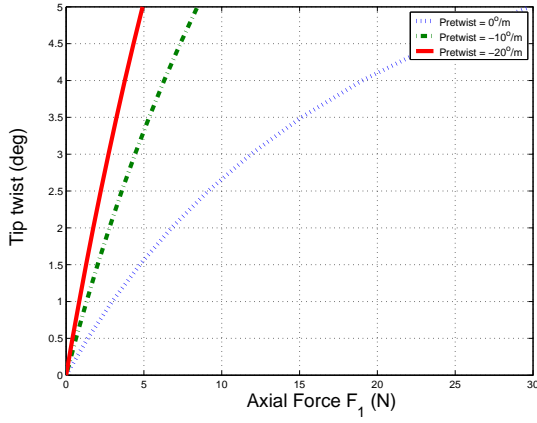


Fig 5. Variation of Twist θ_t with axial force F_1 [$\alpha = 45^\circ$]

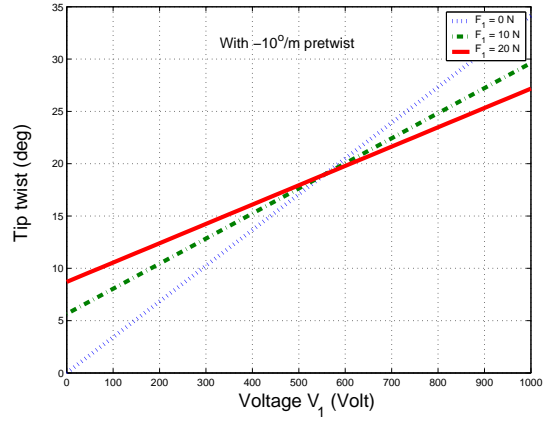


Fig 7. Variation of twist θ_t with voltage V_1 along fibers [$\alpha = 45^\circ$]

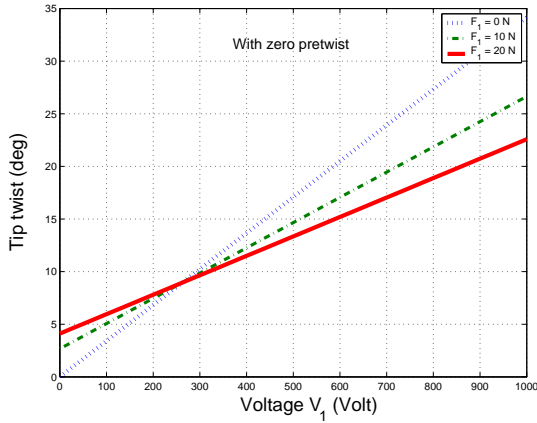


Fig 6. Variation of Twist θ_t with voltage V_1 along fibers [$\alpha = 45^\circ$]

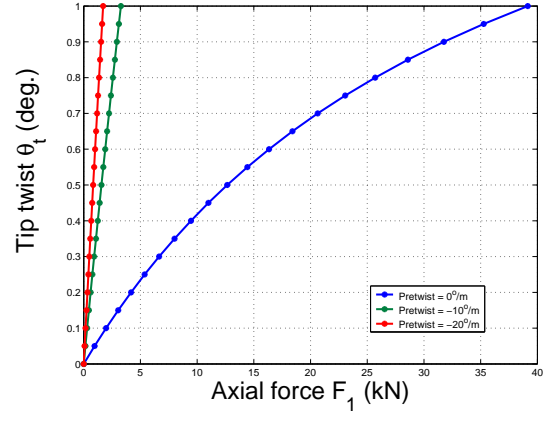


Fig 8. Trapeze effect in a typical tail rotor flex-beam with AFC [$\alpha = 45^\circ$]

comes important to maximize the quantity $\frac{C_1^a}{c_1}$. Fig. 4 shows variation of $\frac{C_1^a}{c_1}$ with fiber orientation angle α . It is clear that $\frac{C_1^a}{c_1}$ is zero for $\alpha = 0^\circ$ and 90° , showing that twist actuation is not possible in cross-ply laminates. Quantity $\|\frac{C_1^a}{c_1}\|$ is maximum at $\alpha \pm 38^\circ$, showing that twist actuation is maximum at $\alpha \pm 38^\circ$. But for practical purposes and ease of manufacturing, $\alpha \approx 45^\circ$ is most suitable. Hence, we consider $\alpha \approx 45^\circ$ for maximum actuation authority in the given laminate.

Fig. 5 shows non-linear coupling between axial force and twist, well known as trapeze effect [15]. With increase in negative pretwist, coupling effect increases. Fig. 6 shows linear variation of twist actuated with actuation voltage V_1 for different values of axial force F_1 . Here, direction of electric field due actuation voltage V_1 is from $x = l$ to $x = 0$. At $V_1=0$, twist is due to trapeze effect. All the plots in Figs. 6-7 pass through a common point of intersection in respective figures. This means that there is a particular actuation electric field, $E_1^a = \frac{(c_3 - \theta_o)c_1}{C_1^a}$ which completely nullifies the trapeze effect. When the voltage corresponding to this electric field is applied, the tip twist remains a constant at $\theta_t = c_3 - \theta_o$, irrespective of the axial force. With increase in axial force F_1 , the slope of actuation curves decrease, showing that actuation authority is reduced. Presence of pretwist along with axial force affects the slope of actuation curves.

Plot in Fig. 6 shows very high actuation authority because of

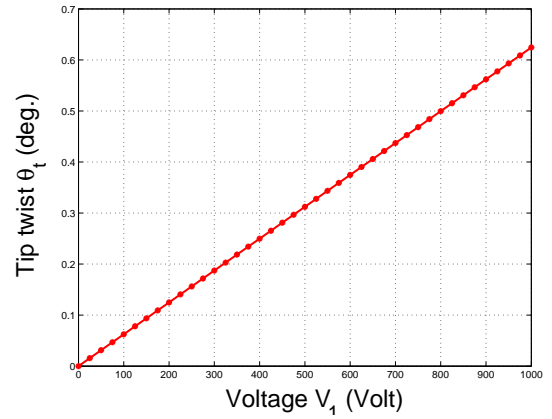


Fig 9. Twist actuation in a typical tail rotor flex-beam with AFC [$\alpha = 45^\circ$]

antisymmetric layup and use of only active AFC layers. Also thickness of the laminate is small. If we include passive layer, (e.g. AS4/3506-1 Graphite/Epoxy, E-glass/Epoxy), actuation authority reduces drastically. For example, consider the thinnest part of a typical tail rotor flex-beam with thickness of 8 mm consisting of 16 plies, each 0.5 mm thick and apply these active layers on the top and bottom of the composite to make [AFC(PZT-5H/Epoxy)+45 degrees/(E-Glass/Epoxy) 0 degrees/AFC (PZT-5H/Epoxy) -45 degrees] laminate with a length $l = 0.318$ m, width $b = 0.07$ m. Material properties of E-Glass/Epoxy lamina are $Q_{11} = 34.059$ GPa, $Q_{12} = 0.3634$ GPa, $Q_{22} = 6.2295$ GPa, $Q_{66} = 2.1945$ GPa. For this flex-beam

configuration, twist actuation results are shown in Figs. 8 and 9, with and without pretwist.

One can observe that twist actuation authority is reduced very much as compared to that of antisymmetric laminate with active layers only. The present theory, when specialized for antisymmetric laminates with no bending and torsion loads, reduces into a very simple form of expression that relates the actuation electric fields with the actuated twist in the laminate in the presence of axial loads.

Conclusion

A variational asymptotic analysis was proposed and then employed to predict the effective stress constants of the AFC laminate. This is the first analysis in the literature to generalize all piezoelectric stress constants of active fiber composites to be non-zero. Expression for strain energy density of an active pretwisted anisotropic strip using piezoelectric fibers of any type of crystal structure have been derived, in which all the components of electric fields are present. This analysis separates the material properties from the external electric field components and produces an easy way to estimate the twist actuation, when electric field is applied in any direction. The analysis is applied for the twist actuation in antisymmetric laminates. In numerical study, it has been proved that twist actuation authority is maximum when piezoelectric fibers are oriented at 38° with strip axis. For the material considered, it is found that twist actuation is possible only by actuation electric field in the direction of the fiber. In the presence of external axial force, actuation authority is decreased. The actuation curves depend upon the sign and magnitude of pretwist and axial force. In the absence axial force, pretwist does not affect twist actuation authority. The main accomplishment of this work was to predict the performance of the generally active fiber composite for the actuation electric field in any possible direction of application. Although the experimental verification of the present work turns out to be beyond the scope of this paper, the presented analysis may provide useful information for optimizing the active fiber composite performance by selecting the optimal microstructure and properties of composite constituents.

Appendix

Expressions for \bar{Q}_{ij}

$$\bar{Q}_{11} = \bar{Q}_{11}^* \cos^2 \theta + 2(\bar{Q}_{12}^* + 2\bar{Q}_{66}^*) \cos^2 \theta \sin^2 \theta + \bar{Q}_{22}^* \sin^4 \theta,$$

$$\bar{Q}_{12} = \frac{1}{8}(\bar{Q}_{11}^* + 6\bar{Q}_{12}^* + \bar{Q}_{22}^* - 4\bar{Q}_{66}^* - (\bar{Q}_{11}^* - 2\bar{Q}_{12}^* + \bar{Q}_{22}^* - 4\bar{Q}_{66}^*) \cos 4\theta),$$

$$\bar{Q}_{16} = \frac{1}{4}(\bar{Q}_{11}^* - \bar{Q}_{22}^* + (\bar{Q}_{11}^* - 2\bar{Q}_{12}^* + \bar{Q}_{22}^* - 4\bar{Q}_{66}^*) \cos 2\theta) \sin 2\theta,$$

$$\bar{Q}_{22} = \bar{Q}_{22}^* \cos^2 \theta + 2(\bar{Q}_{12}^* + 2\bar{Q}_{66}^*) \cos^2 \theta \sin^2 \theta + \bar{Q}_{11}^* \sin^4 \theta,$$

$$\bar{Q}_{26} = -\frac{1}{4}(-\bar{Q}_{11}^* + \bar{Q}_{22}^* + (\bar{Q}_{11}^* - 2\bar{Q}_{12}^* + \bar{Q}_{22}^* - 4\bar{Q}_{66}^*) \cos 2\theta) \sin 2\theta,$$

$$\bar{Q}_{66} = \frac{1}{8}(\bar{Q}_{11}^* - 2\bar{Q}_{12}^* + \bar{Q}_{22}^* + 4\bar{Q}_{66}^* - (\bar{Q}_{11}^* - 2\bar{Q}_{12}^* + \bar{Q}_{22}^* - 4\bar{Q}_{66}^*) \cos 4\theta).$$

Expressions for \bar{e}_{ij}

$$\begin{aligned} \bar{e}_{11} &= \bar{e}_{11}^* \cos^2 \theta - 2\bar{e}_{16}^* \cos \theta \sin \theta + \bar{e}_{21}^* \sin^2 \theta, \\ \bar{e}_{12} &= \bar{e}_{12}^* \cos^2 \theta - 2\bar{e}_{26}^* \cos \theta \sin \theta + \bar{e}_{22}^* \sin^2 \theta, \\ \bar{e}_{16} &= \bar{e}_{16}^* \cos^2 \theta - 2\bar{e}_{66}^* \cos \theta \sin \theta + \bar{e}_{26}^* \sin^2 \theta, \\ \bar{e}_{21} &= \bar{e}_{21}^* \cos^2 \theta + \bar{e}_{11}^* \sin^2 \theta + \bar{e}_{16}^* \sin 2\theta, \\ \bar{e}_{22} &= \bar{e}_{22}^* \cos^2 \theta + \bar{e}_{12}^* \sin^2 \theta + \bar{e}_{26}^* \sin 2\theta, \\ \bar{e}_{26} &= \bar{e}_{26}^* \cos^2 \theta + \bar{e}_{16}^* \sin^2 \theta + \bar{e}_{66}^* \sin 2\theta, \\ \bar{e}_{16} &= \frac{1}{2}(2\bar{e}_{16}^* \cos 2\theta + \bar{e}_{11}^* - \bar{e}_{12}^* \sin 2\theta), \\ \bar{e}_{26} &= \frac{1}{2}(2\bar{e}_{26}^* \cos 2\theta + \bar{e}_{21}^* - \bar{e}_{22}^* \sin 2\theta), \\ \bar{e}_{36} &= \frac{1}{2}(2\bar{e}_{36}^* \cos 2\theta + \bar{e}_{31}^* - \bar{e}_{32}^* \sin 2\theta). \end{aligned}$$

I. Reduced laminate coefficients

Expressions for \bar{A}_{ij} , \bar{B}_{ij} , \bar{D}_{ij}

$$\begin{aligned} \bar{A}_{11} &= A_{11} - \frac{A_{16}^2 A_{22} - 2A_{12} A_{16} A_{26} + A_{12}^2 A_{66}}{A_{22} A_{66} - A_{26}^2}, \\ \bar{B}_{11} &= B_{11} - \frac{-A_{16} A_{26} B_{12} + A_{12} A_{66} B_{12} + A_{16} A_{22} B_{16} - A_{12} A_{26} B_{16}}{A_{22} A_{66} - A_{26}^2}, \\ \bar{B}_{12} &= B_{12} - \frac{-A_{16} A_{26} B_{22} + A_{12} A_{66} B_{22} + A_{16} A_{22} B_{26} - A_{12} A_{26} B_{26}}{A_{22} A_{66} - A_{26}^2}, \\ \bar{D}_{11} &= D_{11} - \frac{A_{66} B_{12}^2 - 2A_{26} B_{12} B_{16} + A_{22} B_{16}^2}{A_{22} A_{66} - A_{26}^2}, \\ \bar{D}_{12} &= D_{12} - \frac{A_{66} B_{12} B_{22} + A_{22} B_{16} B_{26} - A_{26} (B_{16} B_{22} + B_{12} B_{26})}{A_{22} A_{66} - A_{26}^2}, \\ \bar{D}_{22} &= D_{22} - \frac{A_{66} B_{22}^2 - 2A_{26} B_{22} B_{26} + A_{22} B_{26}^2}{A_{22} A_{66} - A_{26}^2}, \\ \bar{B}_{16} &= B_{16} - \frac{-A_{16} A_{26} B_{26} + A_{12} A_{66} B_{26} + A_{16} A_{22} B_{66} - A_{12} A_{26} B_{66}}{A_{22} A_{66} - A_{26}^2}, \\ \bar{D}_{16} &= D_{16} - \frac{A_{66} B_{12} B_{26} + A_{22} B_{16} B_{66} - A_{26} (B_{16} B_{26} + B_{12} B_{66})}{A_{22} A_{66} - A_{26}^2}, \\ \bar{D}_{26} &= D_{26} - \frac{A_{66} B_{22} B_{26} + A_{22} B_{26} B_{66} - A_{26} (B_{26}^2 + B_{22} B_{66})}{A_{22} A_{66} - A_{26}^2}, \\ \bar{D}_{66} &= D_{66} - \frac{A_{66} B_{26}^2 - 2A_{26} B_{26} B_{66} + A_{22} B_{66}^2}{A_{22} A_{66} - A_{26}^2}. \end{aligned}$$

Expressions for \bar{A}_{ij}^a , \bar{B}_{ij}^a

$$\begin{aligned} \bar{A}_{11}^a &= A_{11}^a - A_{12}^a \frac{-A_{16} A_{26} + A_{12} A_{66}}{A_{22} A_{66} - A_{26}^2} - A_{16}^a \frac{A_{16} A_{22} - A_{12} A_{26}}{A_{22} A_{66} - A_{26}^2}, \\ \bar{A}_{21}^a &= A_{21}^a - A_{22}^a \frac{-A_{16} A_{26} + A_{12} A_{66}}{A_{22} A_{66} - A_{26}^2} - A_{26}^a \frac{A_{16} A_{22} - A_{12} A_{26}}{A_{22} A_{66} - A_{26}^2}, \\ \bar{A}_{31}^a &= A_{31}^a - A_{32}^a \frac{-A_{16} A_{26} + A_{12} A_{66}}{A_{22} A_{66} - A_{26}^2} - A_{36}^a \frac{A_{16} A_{22} - A_{12} A_{26}}{A_{22} A_{66} - A_{26}^2}, \\ \bar{B}_{11}^a &= B_{11}^a - A_{16}^a \frac{-A_{26} B_{12} + A_{22} B_{16}}{A_{22} A_{66} - A_{26}^2} - A_{12}^a \frac{A_{66} B_{12} - A_{26} B_{16}}{A_{22} A_{66} - A_{26}^2}, \\ \bar{B}_{21}^a &= B_{21}^a - A_{26}^a \frac{-A_{26} B_{12} + A_{22} B_{16}}{A_{22} A_{66} - A_{26}^2} - A_{22}^a \frac{A_{66} B_{12} - A_{26} B_{16}}{A_{22} A_{66} - A_{26}^2}, \\ \bar{B}_{31}^a &= B_{31}^a - A_{36}^a \frac{-A_{26} B_{12} + A_{22} B_{16}}{A_{22} A_{66} - A_{26}^2} - A_{32}^a \frac{A_{66} B_{12} - A_{26} B_{16}}{A_{22} A_{66} - A_{26}^2}, \\ \bar{B}_{12}^a &= B_{12}^a - A_{16}^a \frac{-A_{26} B_{22} + A_{22} B_{26}}{A_{22} A_{66} - A_{26}^2} - A_{12}^a \frac{A_{66} B_{22} - A_{26} B_{26}}{A_{22} A_{66} - A_{26}^2}, \\ \bar{B}_{22}^a &= B_{22}^a - A_{26}^a \frac{-A_{26} B_{22} + A_{22} B_{26}}{A_{22} A_{66} - A_{26}^2} - A_{22}^a \frac{A_{66} B_{22} - A_{26} B_{26}}{A_{22} A_{66} - A_{26}^2}, \\ \bar{B}_{32}^a &= B_{23}^a - A_{36}^a \frac{-A_{26} B_{22} + A_{22} B_{26}}{A_{22} A_{66} - A_{26}^2} - A_{32}^a \frac{A_{66} B_{22} - A_{26} B_{26}}{A_{22} A_{66} - A_{26}^2}, \\ \bar{B}_{16}^a &= B_{16}^a - A_{16}^a \frac{-A_{26} B_{26} + A_{22} B_{66}}{A_{22} A_{66} - A_{26}^2} - A_{12}^a \frac{A_{66} B_{26} - A_{26} B_{66}}{A_{22} A_{66} - A_{26}^2}, \\ \bar{B}_{26}^a &= B_{26}^a - A_{26}^a \frac{-A_{26} B_{26} + A_{22} B_{66}}{A_{22} A_{66} - A_{26}^2} - A_{22}^a \frac{A_{66} B_{26} - A_{26} B_{66}}{A_{22} A_{66} - A_{26}^2}, \\ \bar{B}_{36}^a &= B_{36}^a - A_{36}^a \frac{-A_{26} B_{26} + A_{22} B_{66}}{A_{22} A_{66} - A_{26}^2} - A_{32}^a \frac{A_{66} B_{26} - A_{26} B_{66}}{A_{22} A_{66} - A_{26}^2}. \end{aligned}$$

II. 1-D stiffness and actuation coefficients

Expressions for S_{ij}

$$\begin{aligned} S_{11} &= b \left(\bar{A}_{11} - \frac{B_{12}^2}{D_{22}} \right), \\ S_{12} &= \frac{b^3 k_1 (-\bar{B}_{12}^2 + \bar{A}_{11} \bar{D}_{22}) + 24b (-\bar{B}_{12} \bar{D}_{22} + \bar{B}_{12} \bar{D}_{26})}{12 \bar{D}_{22}}, \\ S_{13} &= b \bar{B}_{11} - \frac{b \bar{B}_{12} \bar{D}_{12}}{\bar{D}_{22}}, \end{aligned}$$

$$\begin{aligned}
S_{15} &= \frac{b^3}{24} \left(\bar{A}_{11} - \frac{\bar{B}_{12}^2}{D_{22}} \right), \\
S_{22} &= \frac{-3b^5 k_1^2 (\bar{B}_{12}^2 - \bar{A}_{11} \bar{D}_{22}) - 80b^3 k_1 (\bar{B}_{16} \bar{D}_{22} - \bar{B}_{12} \bar{D}_{26})}{240 \bar{D}_{22}} \\
&\quad + \frac{960b(-\bar{D}_{26}^2 + \bar{D}_{22} \bar{D}_{66})}{240 \bar{D}_{22}}, \\
S_{23} &= \frac{b^3 k_1 (-\bar{B}_{12} \bar{D}_{12} - \bar{B}_{11} \bar{D}_{22}) - 24b(\bar{D}_{16} \bar{D}_{22} - \bar{D}_{12} \bar{D}_{26})}{12 \bar{D}_{22}}, \\
S_{25} &= \frac{b^5 k_1 \bar{A}_{11}}{160} - \frac{b^3 \bar{B}_{16}}{12} - \frac{b^5 k_1 \bar{B}_{12}^2}{160 \bar{D}_{22}} + \frac{b^3 \bar{B}_{12} \bar{D}_{26}}{12 \bar{D}_{22}}, \\
S_{26} &= -\frac{b^5 k_1 \bar{B}_{12}^2 \bar{D}_{12}}{360 \bar{D}_{22}} + \frac{b^5 k_1 \bar{A}_{11} \bar{D}_{12}}{360 \bar{D}_{22}}, \\
S_{27} &= -\frac{b^5 k_1 \bar{B}_{12}^3}{360 \bar{D}_{22}} + \frac{b^5 k_1 \bar{A}_{11} \bar{B}_{12}}{360 \bar{D}_{22}}, \\
S_{33} &= b \left(\bar{D}_{11} - \frac{\bar{D}_{12}^2}{D_{22}} \right), \\
S_{35} &= \frac{b^3 \bar{B}_{11}}{24} - \frac{b^7 k_1^2 \bar{B}_{12}^3}{10080 \bar{D}_{22}^2} + \frac{b^7 k_1^2 \bar{A}_{11} \bar{B}_{12}}{10080 \bar{D}_{22}} - \frac{b^3 \bar{B}_{12} \bar{D}_{12}}{24 \bar{D}_{22}} \\
&\quad + \frac{b^5 k_1 \bar{B}_{12}^2 \bar{D}_{26}}{180 \bar{D}_{22}^2} - \frac{b^5 k_1 \bar{A}_{11} \bar{D}_{26}}{180 \bar{D}_{22}}, \\
S_{44} &= \frac{b^3 \bar{A}_{11}}{12} - \frac{b^3 \bar{B}_{12}^2}{12 \bar{D}_{22}}, \\
S_{48} &= \frac{b^5 \bar{B}_{12}^3}{720 \bar{D}_{22}^2} - \frac{b^5 \bar{A}_{11} \bar{B}_{12}}{720 \bar{D}_{22}}, \\
S_{55} &= \frac{b^5 \bar{A}_{11}}{320} - \frac{b^5 \bar{B}_{12}^2}{320 \bar{D}_{22}}, \\
S_{57} &= -\frac{b^5 \bar{B}_{12}^3}{720 \bar{D}_{22}^2} + \frac{b^5 \bar{A}_{11} \bar{B}_{12}}{720 \bar{D}_{22}}, \\
S_{59} &= -\frac{b^7 k_1 \bar{B}_{12}^3}{10080 \bar{D}_{22}^2} + \frac{b^7 k_1 \bar{A}_{11} \bar{B}_{12}}{10080 \bar{D}_{22}} + \frac{b^5 \bar{B}_{12}^2 \bar{D}_{26}}{360 \bar{D}_{22}^2} - \frac{b^5 \bar{A}_{11} \bar{D}_{26}}{360 \bar{D}_{22}}, \\
S_{66} &= -\frac{b^5 \bar{B}_{12}^2 \bar{D}_{12}^2}{720 \bar{D}_{22}^2} + \frac{b^5 \bar{A}_{11} \bar{D}_{12}^2}{720 \bar{D}_{22}^2}, \\
S_{67} &= -\frac{b^5 \bar{B}_{12}^2 \bar{D}_{12}}{720 \bar{D}_{22}^2} + \frac{b^5 \bar{A}_{11} \bar{B}_{12} \bar{D}_{12}}{720 \bar{D}_{22}^2}, \\
S_{69} &= \frac{b^7 k_1 \bar{B}_{12}^3 \bar{D}_{12}}{60480 \bar{D}_{22}^3} - \frac{b^7 k_1 \bar{A}_{11} \bar{B}_{12} \bar{D}_{12}}{60480 \bar{D}_{22}^2} + \frac{b^5 \bar{B}_{12}^2 \bar{D}_{12} \bar{D}_{26}}{360 \bar{D}_{22}^3} \\
&\quad - \frac{b^5 \bar{A}_{11} \bar{D}_{12} \bar{D}_{26}}{360 \bar{D}_{22}^2}, \\
S_{77} &= \frac{b^7 k_1 \bar{B}_{12}^2 (\bar{B}_{12}^2 - \bar{A}_{11} \bar{D}_{22})}{720 \bar{D}_{22}^3}, \\
S_{79} &= \frac{b^7 k_1 \bar{B}_{12}^4}{60480 \bar{D}_{22}^3} - \frac{b^7 k_1 \bar{A}_{11} \bar{B}_{12}^2}{60480 \bar{D}_{22}^2} + \frac{b^5 \bar{B}_{12}^3 \bar{D}_{26}}{360 \bar{D}_{22}^3} - \frac{b^5 \bar{A}_{11} \bar{B}_{12} \bar{D}_{26}}{360 \bar{D}_{22}^2}, \\
S_{88} &= 2 \left(-\frac{b^7 \bar{B}_{12}^4}{15120 \bar{D}_{22}^3} + \frac{b^7 \bar{A}_{11} \bar{B}_{12}^2}{12096 \bar{D}_{22}^2} - \frac{b^7 \bar{A}_{11}^2}{60480 \bar{D}_{22}} \right), \\
S_{99} &= 2 \left[-\frac{31b^9 k_1^2 \bar{B}_{12}^4}{7257600 \bar{D}_{22}^3} + \frac{71b^9 k_1^2 \bar{A}_{11} \bar{B}_{12}^2}{7257600 \bar{D}_{22}^2} - \frac{b^5 \bar{B}_{12}^2 \bar{D}_{12}}{720 \bar{D}_{22}^2} \right. \\
&\quad - \frac{b^9 k_1^2 \bar{A}_{11}^2}{181440 \bar{D}_{22}} + \frac{b^5 \bar{A}_{11} \bar{D}_{12}}{720 \bar{D}_{22}^2} - \frac{b^7 k_1 \bar{B}_{12}^3 \bar{D}_{26}}{30240 \bar{D}_{22}^3} \\
&\quad \left. + \frac{b^7 k_1 \bar{A}_{11} \bar{B}_{12} \bar{D}_{26}}{30240 \bar{D}_{22}^2} - \frac{b^5 \bar{B}_{12}^2 \bar{D}_{12}^2}{360 \bar{D}_{22}^2} + \frac{b^5 \bar{A}_{11} \bar{D}_{26}^2}{360 \bar{D}_{22}^2} \right],
\end{aligned}$$

Others are zero.

Expression for S_{ij}^a

$$\begin{aligned}
S_{11}^a &= \frac{b}{2} \left(\bar{A}_{11}^a - \frac{\bar{B}_{12} \bar{B}_{12}^a}{D_{22}} \right), \\
S_{21}^a &= \frac{b}{2} \left(\bar{A}_{21}^a - \frac{\bar{B}_{12} \bar{B}_{22}^a}{D_{22}} \right), \\
S_{31}^a &= \frac{b}{2} \left(\bar{A}_{31}^a - \frac{\bar{B}_{12} \bar{B}_{32}^a}{D_{22}} \right), \\
S_{12}^a &= \frac{b(b^2 k_1 (-\bar{B}_{12} \bar{B}_{12}^a + \bar{A}_{11}^a \bar{D}_{22}) + 24(-\bar{B}_{16}^a \bar{D}_{22} + \bar{B}_{12}^a \bar{D}_{26}))}{24 \bar{D}_{22}}, \\
S_{22}^a &= \frac{b(b^2 k_1 (-\bar{B}_{12} \bar{B}_{22}^a + \bar{A}_{21}^a \bar{D}_{22}) + 24(-\bar{B}_{26}^a \bar{D}_{22} + \bar{B}_{22}^a \bar{D}_{26}))}{24 \bar{D}_{22}}, \\
S_{32}^a &= \frac{b(b^2 k_1 (-\bar{B}_{12} \bar{B}_{32}^a + \bar{A}_{31}^a \bar{D}_{22}) + 24(-\bar{B}_{36}^a \bar{D}_{22} + \bar{B}_{32}^a \bar{D}_{26}))}{24 \bar{D}_{22}}, \\
S_{13}^a &= \frac{b}{2} \left(\bar{B}_{11}^a - \frac{\bar{B}_{12} \bar{D}_{12}}{D_{22}} \right), \\
S_{23}^a &= \frac{b}{2} \left(\bar{B}_{21}^a - \frac{\bar{B}_{22} \bar{D}_{12}}{D_{22}} \right), \\
S_{33}^a &= \frac{b}{2} \left(\bar{B}_{31}^a - \frac{\bar{B}_{32} \bar{D}_{12}}{D_{22}} \right), \\
S_{14}^a &= \frac{b^3}{48} \left(\bar{A}_{11}^a - \frac{\bar{B}_{12} \bar{B}_{12}^a}{D_{22}} \right), \\
S_{24}^a &= \frac{b^3}{48} \left(\bar{A}_{21}^a - \frac{\bar{B}_{12} \bar{B}_{22}^a}{D_{22}} \right),
\end{aligned}$$

$$\begin{aligned}
S_{34}^a &= \frac{b^3}{48} \left(\bar{A}_{31}^a - \frac{\bar{B}_{12} \bar{B}_{32}^a}{D_{22}} \right), \\
S_{15}^a &= \frac{b^5 k_1}{720} \left(\bar{A}_{11}^a - \frac{\bar{B}_{12}^2}{D_{22}} \right) \frac{\bar{B}_{12}^a}{D_{22}}, \\
S_{25}^a &= \frac{b^5 k_1}{720} \left(\bar{A}_{21}^a - \frac{\bar{B}_{12}^2}{D_{22}} \right) \frac{\bar{B}_{22}^a}{D_{22}}, \\
S_{35}^a &= \frac{b^5 k_1}{720} \left(\bar{A}_{31}^a - \frac{\bar{B}_{12}^2}{D_{22}} \right) \frac{\bar{B}_{32}^a}{D_{22}},
\end{aligned}$$

References

- 1 J. P. Rodger, A. A. Bent and N. W. Hagood, "Characterization of interdigitated electrode piezoelectric fiber composite under high electrical, and mechanical loading," *Proc. society of photo-optical, and instrumentation engineers, San Diego, California.* (1996).
- 2 C. E. S. Cesnik and M. O. Morales, "Active beam cross-sectional modeling," *J. Intelligent Materials and Structures.* 12 (2001) 483-497.
- 3 C. E. S. Cesnik and S. Shin, "On the modeling of integrally actuated helicopter blades," *Int. J. Solids and Structures.* 28(2001) 1765-1789.
- 4 C. E. S. Cesnik and S. Shin, "On the twist performance of multiple-cell helicopter blade," *Smart Materials and Structures.* 1 (1992) 80-83.
- 5 A. A. Bent, N. W. Hagood and J. P. Rodger, "Anisotropic actuation with piezoelectric fiber composites," *J. Intelligent Material System and Structure.* 6 (1995) 338-349.
- 6 A. A. Bent, "Active fiber composites for structural actuation," *PhD Thesis*, MIT, USA. (1997).
- 7 A. J. D. Plessis and N. W. Hagood, "Modeling and experimental testing of twist actuated single cell composite beam for rotor blade control," *A report based on the altered thesis submitted to the Department of Aeronautics and Astronautics in partial fulfillment for the Degree of Master in Science,* MIT, USA. (Feb. 1996).
- 8 J. P. Rodger and N. W. Hagood, "Design manufacturing and testing of an integral twist actuated rotor blade," *8th International Conference on Adaptive Structures and Technology, Wakayama, Japan.* (1992).
- 9 Y. Benveniste and G. J. Dvorak, "Uniform fields and universal relations in piezoelectric composites," *J. Mech. Phys. Solids.* 40(6), (1992) 1295-1312.
- 10 M. L. Dunn and M. Taya, "Micro-mechanics predictions of the effective electroelastic moduli of piezoelectric composite," *J. Solids and Structures.* 30(2) 1993 161-175.
- 11 P. Tan and L. Tong, "Micro-mechanics model for piezoelectric fiber reinforced composite materials," *Composite Science and Technology.* 61 (2001) 759-769.
- 12 A. K. Tamrakar and D. Harursampath, "General constitutive relations for active fiber composites," accepted for publication in *The Third International Conference on Advances in Structural Engineering and Mechanics (ASEM'04), to be held between 2-4 September 2004, Seoul, Korea*
- 13 W. Beckert and S. W. Krecher, "Modeling piezoelectric modules with interdigitated electrode structures," *Computational Material Science* 26 (2003) 36-45.
- 14 P. Tan and L. Tong, "Micro-mechanics model for piezoelectric fiber reinforced composite materials," *Composite Science and Technology* 61 (2001) 759-769.
- 15 D. H. Hodges, D. Harursampath, V. V. Volovoi and C. E. S. Cesnik, "Non-classical effects on non-linear analysis of pretwisted anisotropic strips," *Int. J. Non-Linear Mechanics* 34 (1999) 259-277.
- 16 C. E. S. Cesnik, D. H. Hodges and V. G. Sutyrin, "Cross-sectional analysis of composite beams including large initial twist and curvature effects," *AIAA J.* 34(9) (1996) 1913-1920.
- 17 C. E. S. Cesnik and D. H. Hodges, "VABS: a new concept for composite rotor blade cross-sectional modeling," *J. Amer. Helicopter Soc.* 42 (1997) 27-38.
- 18 D. A. Danielson and D. H. Hodges, "Non-linear beam kinematics by decomposition of the rotation tensor," *J. Appl. Mech.* 54 (1987) 258-262.
- 19 V. G. Sutyrin and D. H. Hodges, "On asymptotically correct linear laminated plate theory," *Int. J. Solids and Structures.* 33 (1996) 3649-3671.
- 20 Berdichevskii V. L., "Variational-asymptotic method of shell theory construction," *PMM.* 34 (1979) 664-687.
- 21 D. A. Danielson and D. H. Hodges, "A beam theory for large global rotation, moderate local rotation, and small strain," *J. Appl. Mech.* 55 (1988) 179-184.